DNA Nanotechnology

DOI: 10.1002/anie.200903319

Template-Directed Nucleation and Growth of Inorganic Nanoparticles on DNA Scaffolds**

Linda A. Stearns, Rahul Chhabra, Jaswinder Sharma, Yan Liu, William T. Petuskey, Hao Yan, and John C. Chaput**

Structural DNA nanotechnology provides a robust method for building nanoscale molecules that self-assemble into structures that resemble their original design. Since inception, this technology has produced numerous two- and three-dimensional objects, including planar arrays, cylindrical tubes, and various geometric shapes.[1,2] The ability of this method to create programmable surfaces with addressable features provides a unique opportunity to design synthetic scaffolds that control the spatial orientation of individual molecules in precise nanoscale dimensions. One of the more exciting applications that this technology can permit is the design of inorganic nanostructures that assemble multiple inorganic components on a single surface.[3] While thiol-modified oligonucleotides have been used extensively to assemble preformed gold nanoparticles (NPs) on DNA nanostructures,[4] more general strategies are now needed to expand the versatility of the DNA scaffold to other types of inorganic NPs.

One way to bridge the gap between structural DNA nanotechnology and future nanoscale inorganic materials is to exploit the molecular recognition properties of inorganic-binding peptides (IBPs). These are peptides with affinity to inorganic surfaces, including metals, semiconductors, and metal oxides, that have been identified by biological design and test-tube evolution methods.[5–8] Remarkably, some IBPs show biomineralizing activity and are able to reduce soluble metal ions to insoluble metal particles with discrete sizes and shapes.[9–11] Despite significant advances in structural DNA nanotechnology, no examples currently exist in which inorganic-binding peptides have been integrated into DNA nanostructures for the purpose of controlling the spatial positioning of inorganic NPs on the nanoscale. Herein, we describe the design and synthesis of self-assembled inorganic nanostructures in which peptides immobilized on the surface of a DNA nanotube are used to template-direct the in situ nucleation and growth of gold nanoparticles from soluble chemical precursors.

Peptide A3 was selected by phage display to bind silver nanoparticles.[10] Functional characterization revealed that this amino acid sequence recognizes both silver and gold surfaces and is capable of reducing soluble silver and gold ions to their metallic forms.[11] Gold NPs formed by this peptide have a discrete size of 8–10 nm. While the precise mechanism of NP nucleation and growth is unclear, early indications suggested that electron transfer to $AuCl_4^-$ (the soluble gold form used in this reaction) occurred by the reduction of a tyrosine side chain in the amino acid sequence to phenoxide.[14] More recent studies indicate that the gold NPs result from a reaction between soluble gold ions and the HEPES buffer (4-(2-hydroxyethyl)-1-piperazine-ethanesulfonic acid) used in the biomineralization step[12] and that the peptide controls the site of nucleation. According to this premise, peptide A3 was used as a nucleation agent for distributing gold NPs on a synthetic scaffold assembled from peptide amphiphiles.[13]

Intrigued by the possibility of using DNA origami techniques to build inorganic nanostructures with programmable features, we constructed a DNA scaffold that assembled single-stranded M13 viral DNA into a six-helix bundle with the shape of a nanotube.[14] The nanostructure was designed to identify 168 helper strands of DNA (Supporting Information Table 1) that anneal to different regions of the viral template and allow the DNA to fold into a tube that spans a length of 380 nm. Ten of the 168 helper strands contained unpaired single-stranded regions that could be used as addressable locations for annealing the A3 peptide that was conjugated to a DNA tag (Supporting Information Table 2). The process of displaying peptides on the surfaces of DNA scaffolds is referred to as nanodisplay; this technique has been used previously to construct high-density peptide and antibody-capture nanoarrays.[15]

We began by conjugating the A3 peptide to a short DNA tag using standard amine coupling chemistry.[16] The resulting peptide–DNA conjugate was then annealed in a HEPES-buffered solution to complementary DNA capture probes present on the surface of preformed DNA nanotubes (Figure 1). Formation of the DNA nanotube was verified

[*] L. A. Stearns, Prof. J. C. Chaput
Center for BioOptical Nanotechnology, The Biodesign Institute and Department of Chemistry and Biochemistry
Arizona State University, Tempe, AZ 85287 (USA)
Fax: (+1) 480-727-0396
E-mail: john.chaput@asu.edu
R. Chhabra, J. Sharma, Prof. Y. Liu, Prof. H. Yan
Center for Single Molecule Biophysics, The Biodesign Institute and Department of Chemistry and Biochemistry
Arizona State University, Tempe, AZ 85287 (USA)
Fax: (+1) 480-727-2378
E-mail: hao.yan@asu.edu
Prof. W. T. Petuskey
Department of Chemistry and Biochemistry
Arizona State University, Tempe, AZ 85287 (USA)

[**] This work was supported by a grant from the Office of Naval Research (N000140710194G) to H.Y. and J.C.C. We gratefully acknowledge use of facilities in the Leroy Eyring Center for Solid State Science (CSSS) at ASU.

Supporting information for this article is available on the WWW under http://dx.doi.org/10.1002/anie.200903319.

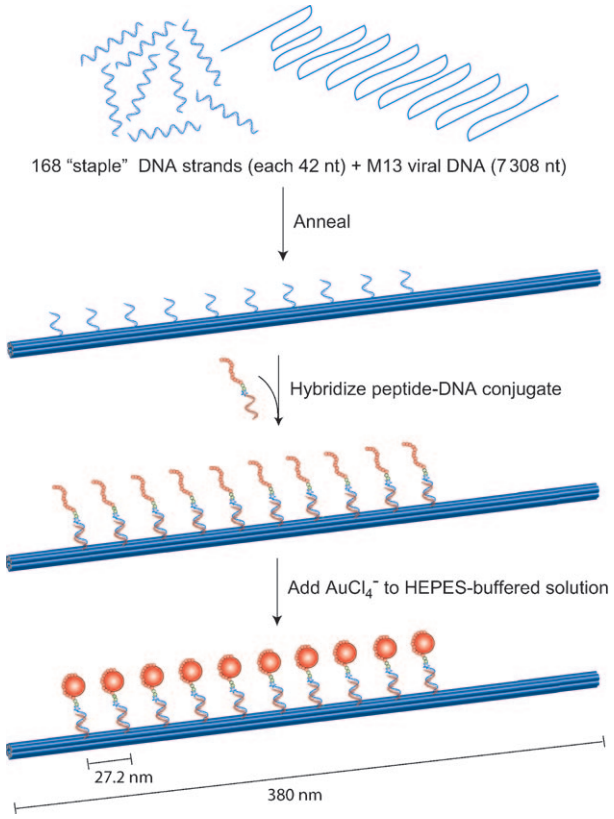

Figure 1. The six-helix bundle nanotube is self-assembled by annealing 168 staple DNA strands with the M13 viral DNA. The nanotube was designed to display ten single-stranded DNA capture probes to which the complementary peptide–DNA conjugate is hybridized. In the final step, soluble $AuCl_4^-$ is added to the HEPES-buffered solution to initiate gold nanoparticle nucleation and growth. HEPES = 4-(2-hydroxyethyl)-1-piperazineethanesulfonic acid, nt = nucleotide.

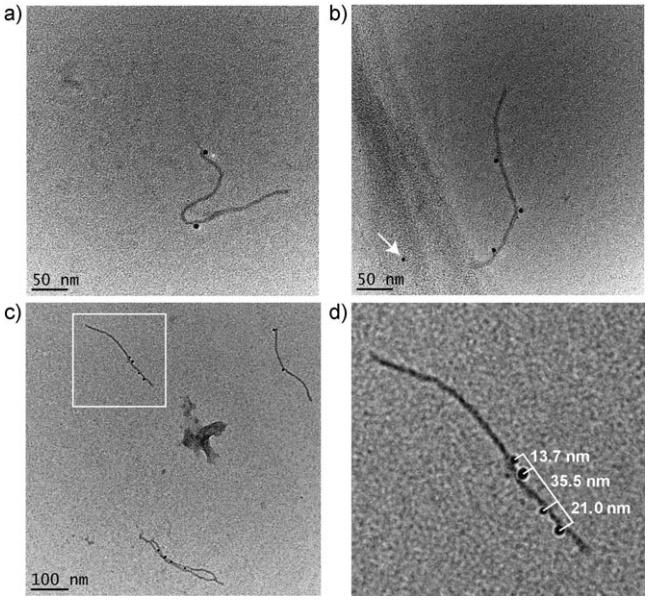

Figure 2. TEM micrographs of peptide-modified nanotubes displaying bound gold nanoparticles. The NPs were prepared by in situ nucleation and growth from HEPES buffer and $AuCl_4^-$. a, b) Isolated nanotubes display two and three NPs, respectively. An arrow marks the position of a free NP that is not localized to any nanotube. c) A typical distribution of nanotubes displaying (clockwise from top left) four, two, and four nanoparticles, respectively. d) Inset from Figure 2c shows interparticle distances for a single nanotube.

before and after annealing by atomic force microscopy (Supporting Information Figure 1). Annealing was performed using a three-fold molar excess of peptide–DNA conjugate to ensure complete hybridization to the DNA nanotube. After hybridization, soluble gold ions were added to the solution to initiate the nucleation and growth of 5–10 nm gold NPs at locations where the peptide was displayed on the surface of the DNA nanotube. Within 1–2 min, the reaction mixture turned a reddish-black color, indicating that gold NPs had formed.

We used transmission electron microscopy (TEM) with DNA staining to verify the presence of gold NPs on the surface of the DNA nanotube. The resulting images (Figure 2 and Figure 3) showed that the gold NPs were located at the DNA nanotube surface. Very few NPs were observed as free-floating particles independent of the nanotubes. TEM images (Supporting Information Figure 2) of control experiments in which gold ions were added directly to the HEPES buffer or to HEPES buffer containing the DNA nanotube but no peptide demonstrated that although gold NPs formed in the absence of the A3 peptide, these particles were randomly distributed throughout the images. Taken together, these experiments demonstrate the importance of the A3 peptide in controlling the site of NP formation. While the actual mechanism of NP formation is not yet known, it is possible that the peptide provides a stable nucleation site by coordinating to the initial metal cluster during the early steps of nanoparticle nucleation and growth.

In our template-directed nucleation experiments, we observed two types of inorganic DNA nanostructures when gold ions were added to the solution. The first structure was our designed inorganic-modified DNA nanotube (Figure 2) in which gold nanoparticles segregated to individual DNA nanotubes. A representative sampling indicated that these structures contained an average of two to three gold NPs per DNA nanotube, with a maximum of five imaged on a single tube. The nanoparticles were largely spherical and monodisperse, ranging from 4.7 to 9.7 nm in diameter, with an average particle size of 6.6 nm ($n = 48$, standard deviation 1.1 nm). Our efforts to increase NP density by elevating the concentration of the soluble gold ions in solution produced only large NP aggregates and nanotubes without NPs (Supporting Information Figure 3). Only rarely did we observe isolated NPs that were not attached to any DNA nanotube (Figure 2b, arrow). These NPs may have formed from excess peptide–DNA conjugate used in the annealing step. Given the relatively sparse distribution of free NPs observed throughout our images, it is possible that free peptide–DNA conjugates may have formed NPs that subsequently aggregated and evaded detection by TEM.

In instances where the nanotube contained multiple NPs, nanoparticles were generally not distributed at the designed 27 nm intervals, likely owing to the flexibility of the tethered peptide or to attractive forces between adjacent NPs. For multiple, consecutive NPs on a linear nanotube, the closest interparticle distance averaged 13.4 nm. For the gold-deco-

rated nanotube in Figure 2 d, this distance was 13.7 nm, which is roughly one-half of the 27 nm spacing defined by the DNA capture strands (Figure 1). In this case, van der Waals attractive forces may have favored the positioning of gold NPs between adjacent peptide strands. This explanation is consistent with the length of the peptide and DNA capture probe sequence. Attractive forces between the nanotube-bound gold NPs and TEM grid may have also influenced the observed nanoparticle positions.

The second type of inorganic nanostructure observed in our in situ synthesis experiments were multimeric nanostructures that combined two or more nanotubes with gold NPs located along the interface between the tubes. Representative images are shown in Figure 3. The frequent occurrence of NPs at locations where multiple nanotubes intersect suggests that more than one peptide may be required to promote effective gold nanoparticle nucleation. This hypothesis is supported by the work of Rosi and co-workers, whose A3-derivatized peptide nanoribbons served as an efficient scaffold for gold nanoparticle nucleation and growth.[13] Whereas peptide–peptide interactions provided the framework for the Rosi group's nanostructures, the designed interpeptide spacing (27 nm) on our DNA nanotube was likely too large to effectively facilitate interactions between neighboring peptides. This effect could account for the reduced efficiency of NP nucleation on our DNA scaffold compared to the Rosi group's peptide nanoribbons. However, in cases where multiple DNA nanotubes intersect, we do observe large numbers of gold NPs, which could be due to multiple peptides interacting synergistically. Despite the observation that multiple peptides may provide a more efficient nucleation site, it is clear from our data that a single peptide is sufficient to nucleate a gold nanoparticle.

Because many self-assembly strategies utilize thiol-modified DNA strands to capture preformed gold nanoparticles on DNA nanostructures, we explored the use of preformed gold NPs capped with bis(*p*-sulfonatophenyl)phenylphosphine as a source of gold NPs for our inorganic-modified DNA nanotube. In these experiments, nanotubes were assembled as described in Figure 1, and the A3 peptide was used to capture suspended gold NPs. TEM images of these samples failed to show any convincing evidence that the NPs were regularly distributed on the nanotube. This result suggests that the A3 peptide is a weak ligand for gold and therefore unable to effectively displace the phosphine cap used to solubilize the gold NPs. It also suggests that peptides with higher affinities for gold might yield more extensive inorganic nanostructures. Rosi and co-workers observed a similar result when the A3 peptide was incorporated into an amphiphilic scaffold.[13]

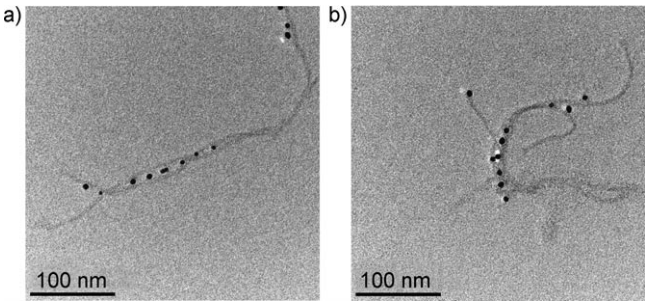

Figure 3. TEM micrographs of peptide-modified nanotubes displaying bound gold nanoparticles. a, b) Multimeric nanostructures are observed when multiple nanotubes converge on the same series of NPs.

In summary, we present a new paradigm for creating inorganic nanomaterials that relies on the molecular recognition properties of inorganic-binding peptides to direct the in situ nucleation and growth of inorganic nanoparticles at addressable locations on a DNA scaffold. Using nanodisplay, a method for presenting polypeptide sequences on DNA nanostructures, we prepared a DNA nanotube containing gold-binding peptides capable of nucleating nanoparticles of a discrete size (5–10 nm) from soluble chemical precursors. The resulting inorganic nanostructure represents an important step forward in the synthesis of programmable inorganic materials by self-assembly methods.

Received: June 19, 2009
Revised: July 30, 2009
Published online: September 30, 2009

Keywords: DNA · inorganic nanostructures · inorganic-binding peptides · nanoparticles · nanotechnology

[1] P. W. K. Rothemund, *Nature* **2006**, *440*, 297 – 302.
[2] a) N. C. Seeman, *Nature* **2003**, *421*, 427 – 431; b) F. A. Aldaye, A. L. Palmer, H. F. Sleiman, *Science* **2008**, *321*, 1795 – 1799; c) C. Lin, Y. Liu, H. Yan, *Biochemistry* **2009**, *48*, 1663 – 1674.
[3] N. C. Seeman, A. M. Belcher, *Proc. Natl. Acad. Sci. USA* **2002**, *99*, 6451 – 6455.
[4] a) J. D. Le, Y. Pinto, N. C. Seeman, K. Musier-Forsyth, T. A. Taton, R. A. Kiehl, *Nano Lett.* **2004**, *4*, 2343 – 2347; b) J. Zheng, P. E. Constantinou, C. Micheel, A. P. Alivisatos, R. A. Kiehl, N. Seeman, *Nano Lett.* **2006**, *6*, 1502; c) J. Sharma, R. Chhabra, A. Cheng, J. Brownell, Y. Liu, H. Yan, *Science* **2009**, *323*, 112 – 116; d) J. Sharma, R. Chhabra, Y. Liu, Y. Ke, H. Yan, *Angew. Chem.* **2006**, *118*, 744; *Angew. Chem. Int. Ed.* **2006**, *45*, 730; e) J. Sharma, R. Chhabra, C. S. Andersen, K. V. Gothelf, H. Yan, Y. Liu, *J. Am. Chem. Soc.* **2008**, *130*, 7820 – 7821.
[5] U. Kriplani, B. K. Kay, *Curr. Opin. Biotechnol.* **2005**, *16*, 470 – 475.
[6] B. R. Peelle, E. M. Krauland, K. D. Wittrup, A. M. Belcher, *Langmuir* **2005**, *21*, 6929 – 6933.
[7] M. Sarikaya, C. Tamerler, A. K-Y. Jen, K. Schulten, F. Baneyx, *Nat. Mater.* **2003**, *2*, 577 – 585.
[8] R. L. Willett, K. W. Baldwin, K. W. West, L. N. Pfeiffer, *Proc. Natl. Acad. Sci. USA* **2005**, *102*, 7817 – 7822.
[9] C. E. Flynn, C. Mao, A. Hayhurst, J. L. Williams, G. Georgiou, B. Iverson, A. M. Belcher, *J. Mater. Chem.* **2003**, *13*, 2414 – 2421.
[10] R. R. Naik, S. J. Stringer, G. Agarwal, S. E. Jones, M. O. Stone, *Nat. Mater.* **2002**, *1*, 169 – 172.
[11] J. M. Slocik, M. O. Stone, R. R. Naik, *Small* **2005**, *1*, 1048 – 1052.
[12] J. Xie, J. Y. Lee, D. I. C. Wang, *Chem. Mater.* **2007**, *19*, 2823 – 2830.
[13] J-L. Chen, P. Zhang, N. L. Rosi, *J. Am. Chem. Soc.* **2008**, *130*, 13555 – 13557.
[14] S. M. Douglas, J. J. Chou, W. M. Shih, *Proc. Natl. Acad. Sci. USA* **2007**, *104*, 6644 – 6648.
[15] B. A. R. Williams, K. Lund, Y. Liu, H. Yan, J. C. Chaput, *Angew. Chem.* **2007**, *119*, 3111 – 3114; *Angew. Chem. Int. Ed.* **2007**, *46*, 3051 – 3054.
[16] J. G. Harrison, S. Balasubramanian, *Nucleic Acids Res.* **1998**, *26*, 3136 – 3145.

